

NMR studies of proton transfer in 1:1 tris(trimethoxyphenyl)-phosphine oxide–phenol complexes



Claudia M. Lagier,^a Alejandro C. Olivieri^{*a} and Robin K. Harris^{*b}

^a Departamento de Química Analítica, Facultad de Ciencias Bioquímicas y Farmacéuticas, Universidad Nacional de Rosario, Suipacha 531, Rosario 2000, Argentina

^b Department of Chemistry, University of Durham, South Road, Durham, UK DH1 3LE

The hydrogen transfer process in adducts between tris(trimethoxyphenyl)phosphine oxide (TMPPPO) and eight different substituted phenols has been studied in both the solution and solid states. For this purpose, ¹H and ³¹P NMR solution-state spectra of these complexes have been recorded. The ¹H chemical shift of the hydrogen-bonded proton and the ³¹P chemical shift of the phosphine oxide are largely influenced by the substituents attached to the phenol. Thus, the chemical shift of the hydroxylic hydrogen for complexes in solution varies from lower frequencies (8.2 ppm) for phenol derivatives of high p*K*_a (e.g. 10.2) to higher frequencies (11.9 ppm) as the p*K*_a of the phenol decreases. However, for highly acid phenols such as picric acid (p*K*_a = 0.38), the signal moves to lower frequencies again as a result of the shielding produced by the oxygen atom of the TMPPPO residue. On the other hand, the ³¹P chemical shift of the complexes in solution varies with the same trend: as the p*K*_a of the substituted phenol decreases, the phosphorus signal moves to higher frequencies. The eight complexes have also been studied in the solid state by means of high-resolution CPMAS ¹³C and ³¹P NMR experiments. There is also evidence of the hydrogen transfer process in the solid state which causes changes in the ³¹P shielding tensor, and in the ¹³C chemical shifts of the phenolic C–O (C1) and *para* (C4) carbons. In spite of crystallographic packaging effects that might occur in the solid phase, the results parallel those obtained for complexes in solution, since the two sets of NMR data follow almost the same pattern.

Introduction

NMR spectroscopy has proved to be a useful tool to study hydrogen transfer processes for many systems.^{1–8} Among the systems that have been examined by this technique are the complexes in which substituted phenols form the acid that donates the proton, and an amine or phosphine oxide is the base that accepts it.^{9–14}

It has been found that, for these systems in solution, a correlation exists between the strength of the phenol as proton donor and the ¹H chemical shift of the hydroxylic hydrogen.^{15–17}

In a previous study, we examined complexes between triphenylphosphine oxide (TPPO) and substituted phenols not only in solution but also in the solid state.¹⁴ A correlation between the p*K*_a of the phenol and the degree of hydrogen transfer was found for these complexes in solution. However, the same study performed on these adducts in the solid state showed only a very weak correlation. This behaviour was attributed mainly to the fact that TPPO is a weak base, and crystallographic influences obscure the effect of the acid–base reaction that occurs for the complexes in solution.¹⁴ Taking this fact into account, it seemed to be of interest to perform an analogous study in systems where the residue accepting the proton was a more basic oxide. Therefore, the oxide of a highly basic phosphine,¹⁸ tris(2,4,6-trimethoxyphenyl)phosphine oxide (TMPPPO), was prepared in order to study the hydrogen transfer process for complexes with substituted phenols, not only in solution but also in the solid phase.

First, these adducts were examined in solution by means of ¹H and ³¹P NMR spectroscopy to verify the presence of a hydrogen-transfer process. Then, the complexes were studied in the solid state by means of ¹³C NMR, according to the following treatment.

On the basis of a tautomeric equilibrium for a phenol complex such as eqn. (1), X being a nitrogen or phosphorus atom, it



has been proved that carbons at positions 1 and 4 of the phenol are affected strongly by the strength of the hydrogen bond involved.^{12–17} Hence, it has been useful to calculate the double difference between the C1 and C4 chemical shifts for the substituted phenol when it takes part in the complex, and when there is no acid–base reaction (e.g. in the pure phenol) according to eqn. (2).¹⁶ The difference Δ_{1-4} has been used as a measure of

$$\Delta_{1-4} = [\delta_{\text{C1}} - \delta_{\text{C4}}]_{\text{phenol-base}} - [\delta_{\text{C1}} - \delta_{\text{C4}}]_{\text{phenol}} \quad (2)$$

the state of reaction (1), in terms of the degree of proton transfer to the base residue.^{14,16,17} The use of eqn. (1), in circumstances where NMR cannot distinguish two situations for any particular case, is justified whether there is a double-well potential with exchange that is rapid on the NMR timescale or a single-well potential.

The solid complexes have also been studied by means of ³¹P NMR spectroscopy, taking advantage of the modifications that the shielding tensor experiences with regard to minor changes in the electronic environment of the phosphorus nucleus. In this type of compound, the ³¹P tensor is expected to be highly sensitive to even slight changes in chemical bonding, since the hydrogen bond involved in the transfer is separated by only one oxygen atom from the observed nucleus.

Experimental

Tris(2,4,6-trimethoxyphenyl)phosphine (TMPP) was purchased from Aldrich. Five grams of TMPP were dissolved in dichloromethane in a one-neck round-bottomed flask; 5 ml of hydrogen peroxide (100 volumes) was added and stirred for 6 h. The organic fraction was then obtained by means of a separating funnel and the aqueous layer was extracted twice with 15 ml of dichloromethane. The organic fractions were combined and washed three times with water, to be finally dried over sodium sulfate. Crystals of TMPPPO were obtained by slow evaporation

of the solvent. The product was recrystallised from a mixture of dichloromethane–hexane, also by slow evaporation. White crystals were exposed to high vacuum for several hours to fully dehydrate the material. Elemental analysis and ^1H , ^{13}C and ^{31}P NMR spectra of the product in solution showed TMPPO was free from impurities.

All phenols were of the highest analytical grade commercially available. 1:1 stoichiometric amounts of each substituted phenol and TMPPO were dissolved in chloroform. Crystals of the corresponding complexes were obtained by slow evaporation of the solvent, and the recovered adducts were dried under high vacuum for 12 h.

Solutions of the complexes were prepared for ^1H NMR spectra with $[\text{D}_2]\text{chloroform}$, which was dried over a 3 Å molecular sieve. The ^1H NMR spectra were recorded at room temperature (*ca.* 20 °C) on a Bruker AC 200 NMR spectrometer operating at 200.1 MHz nominal frequency, and using tetramethylsilane (TMS) as internal standard for the chemical shifts. The typical operating conditions were: number of transients 128; recycle delay 1 s; pulse duration 2 μs (7.2 $\mu\text{s} \equiv 90^\circ$); acquisition time 1.5 s.

Phosphorus-31 NMR spectra were obtained from $[\text{D}_2]\text{chloroform}$ solutions at room temperature (*ca.* 20 °C) on a Varian VXR 400S spectrometer operating at 161.9 MHz nominal frequency, and with ^1H high-power decoupling during acquisition. Signals were referenced against an 85% aqueous solution of phosphoric acid. The spectrometer parameters were as follows: number of transients 64; recycle delay 1 s; pulse duration 6 μs ; acquisition time 3.0 s.

A Chemagnetics CMX200H NMR spectrometer was used to record the solid-state ^{13}C and ^{31}P NMR spectra. The respective operating frequencies were 50.3 and 80.0 MHz. Both sets of spectra were acquired using the CPMAS technique with high-power proton decoupling. Carbon-13 NMR spectra were recorded under the following operating conditions: number of transients 1200–8000; recycle delay 2–10 s; pulse duration 4 μs (90°); contact time 3.0–5.0 ms; acquisition time: 51–102 ms; spectral width 20 kHz. The adamantane signal ($\delta_{\text{CH}_2} = 38.4$ ppm with respect to TMS) was used as a secondary reference for the ^{13}C chemical shifts. The ^{31}P NMR operating conditions were: number of transients 16–80; pulse duration 5 μs (90°); contact time 2.5–5.0 ms; acquisition time 20–61 ms; spectral width 30–50 kHz. The brushite signal ($\delta_{\text{iso}} = 1.2$ ppm with respect to 85% aqueous phosphoric acid) was used as a secondary reference for the solid-state phosphorus-31 spectra. The sample spinning speeds ranged from 0.8 to 2.8 kHz to obtain an appropriate number of spinning sidebands. The method of Fenzke *et al.*¹⁹ was used to retrieve the principal components of the ^{31}P shielding tensor components, using a computer program which also calculates errors in the values.²⁰

Results and discussion

Solution studies

A summary of the NMR results obtained from chloroform solution at room temperature (*ca.* 20 °C) for ^1H chemical shifts of the hydroxylic hydrogen for TMPPO complexes, together with phosphorus-31 chemical shift values of adducts, is presented in Table 1. It should be noticed that the whole set of solutions to record ^1H NMR spectra was prepared in a dry atmosphere. This was necessary to eliminate the presence of water, which would exchange hydrogen atoms rapidly, leading to average chemical shift values. The relevant results of ^1H NMR measurements for substituted phenol–TMPPO adducts as a function of the $\text{p}K_{\text{a}}$ of the phenols are presented in Fig. 1. The changes in proton chemical shifts in hydrogen-bonded systems are a consequence of the low electron density arising from the interaction between the observed hydrogen and both oxygen atoms near to it. For complexes in which weak acid phenols are the hydrogen donors, the ^1H signal gives a relatively low chem-

Table 1 Solution-state phenolic ^1H and ^{31}P chemical shifts of TMPPO–phenol complexes, together with the $\text{p}K_{\text{a}}$ values of the pure phenols

Compound	$\text{p}K_{\text{a}}$	Adducts $\delta^1\text{H}(\text{HO})$ (ppm)	Adducts $\delta^{31}\text{P}$ (ppm)
Picric acid ^a	0.38	7.4	39.5
2,6-Dichloro-4-nitrophenol	3.70	—	13.9
2,6-Dinitrophenol	3.71	11.3	11.1
2,4-Dinitrophenol	3.96	11.5	16.1
2,5-Dinitrophenol	5.22	11.9	14.8
4-Nitrophenol	7.15	11.4	14.8
4-Chlorophenol	9.37	9.1	12.4
Phenol	9.89	8.4	11.9
4-Methoxyphenol	10.21	8.2	13.5

^a Picric acid is 2,4,6-trinitrophenol.

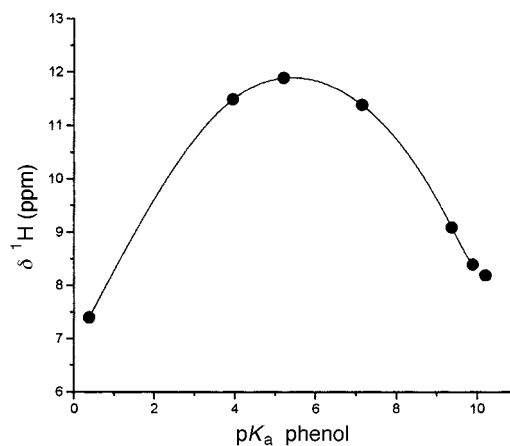


Fig. 1 Hydroxylic ^1H chemical shifts for phenol–TMPPO complexes in solution as a function of $\text{p}K_{\text{a}}$ for the phenol

ical shift. As the $\text{p}K_{\text{a}}$ of the phenol decreases, the hydrogen signal involved first shifts to higher frequencies, presenting a maximum for the 2,5-dinitrophenol–TMPPO system. This change is the expected one, taking into account that, for weak acids, the hydrogen nucleus is near the oxygen atom of the phenol and, consequently, the signal appears at relatively low frequencies. As the acid strength of the substituted phenol increases, the hydrogen nucleus involved moves away from the phenolic oxygen, enlarging its deshielding. This phenomenon proceeds until the hydrogen nucleus is substantially transferred to the base moiety, when it again begins to exhibit a relatively lower chemical shift due to the vicinity of the TMPPO oxygen atom. In the case of the picric acid complex, the hydroxylic ^1H chemical shift is displaced to significantly lower frequencies. It should be noticed that no signal for the hydroxylic proton could be found in the 2,6-dichloro-4-nitrophenol derivative, presumably due to the presence of traces of water dramatically broadening the relevant ^1H signal. However, this complex was studied by means of ^{31}P NMR experiments.

Table 1 also displays solution $\delta^{31}\text{P}$ values determined for the adducts studied. It can be seen that the hydrogen transfer process can be monitored by the ^{31}P chemical shift as a function of $\text{p}K_{\text{a}}$ of the substituted phenol. For these compounds, as long as the phenol is not a strong hydrogen donor, the phosphorus-31 nucleus has a chemical shift similar to that observed for pure TMPPO (13.90 ppm). However, as proton transfer from the phenol to the base takes place, structures in which phosphorus has an increased positive charge arise. This fact leads to an increasing deshielding of phosphorus nucleus for lower $\text{p}K_{\text{a}}$ values of the substituted phenol. The highest observed chemical shift is 39.50 ppm for the picric acid–TMPPO adduct, where the $\text{p}K_{\text{a}}$ of the phenol involved is 0.38. However, for phenols that are weaker acids than picric acid and

Table 2 Relevant high-resolution solid-state ^{13}C NMR data for pure phenols and TMPPO–phenol complexes

Compound	Pure phenols		Complexes		Δ_{1-4}^a (ppm)
	δ_{C1} (ppm)	δ_{C4} (ppm)	δ_{C1} (ppm)	δ_{C4} (ppm)	
Picric acid	155.0	137.3	162.0	128.2	21.2
2,6-Dichloro-4-nitrophenol	155.9	140.6	157.5	138.6	3.6
2,6-Dinitrophenol	152.3	120.8	149.0	118.1	4.5
2,4-Dinitrophenol	159.1	140.2	168.1	137.2	17.1
2,5-Dinitrophenol	154.9	114.7	157.8	115.4	7.3
4-Nitrophenol	163.3	141.3	168.0	139.3	6.7
4-Chlorophenol ^b	152.9	125.4	158.2	123.0	7.7
Phenol	154.6	121.3	158.8	119.4	6.1
4-Methoxyphenol	150.0	154.6	151.4	153.7	2.3

^a These values were calculated using the experimental solid-state ^{13}C NMR data of the substituted phenols and of the complexes. Corrections were made for the 2- and 6-nitro-substituted phenols according to the procedure described in refs. 9 and 17 (see text). ^b *para*-Carbon-13 for the pure phenol gave two signals (splitting 8.4 ppm) as a consequence of residual dipolar coupling to quadrupolar $^{35/37}\text{Cl}$ nuclei.^{33,34} δ_{C4} has been calculated as the weighted average of this doublet.

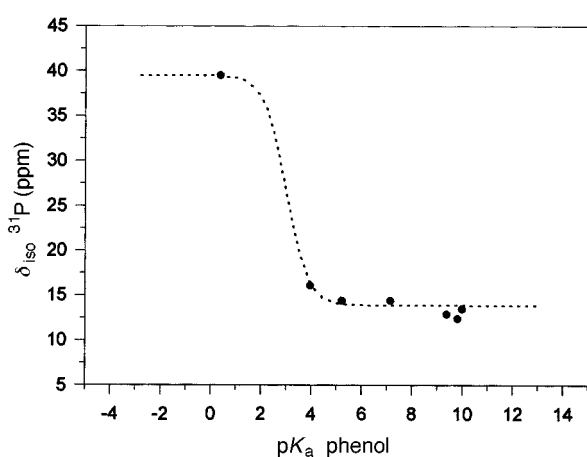


Fig. 2 Phosphorus-31 chemical shift for the complexes in solution as a function of $\text{p}K_{\text{a}}$ of the phenol. The dotted line represents the sigmoidal theoretically calculated according to eqn. (3). The filled circles are the $\delta^{31}\text{P}$ experimentally observed.

have two bulky substituents in positions 2 and 6 simultaneously, it seems there is no hydrogen transfer. Examination of the ^{31}P chemical shift for the 2,6-dichloro-4-nitrophenol–TMPPO system (13.92 ppm) shows the effect mentioned since this value is nearly the same as that recorded for pure TMPPO. A possible explanation for this fact is that steric hindrance prevents the hydroxylic proton from being close enough to TMPPO to allow the acid–base reaction to take place. This seems to be also the case for the 2,6-dinitrophenol–TMPPO system, which has a ^{31}P chemical shift of the same order as for pure TMPPO. The same phenomenon has already been described for complexes between the latter phenol and triphenylphosphine oxide (TPPO) in the solid state.¹⁴ In this case, TMPPO has substituents that are more bulky than TPPO, and it seems possible that the effect described could be displayed even in the solution state.

Eqn. (3) describes the theoretical sigmoidal curve for which

$$\delta^{31}\text{P} = \frac{13.9 + 39.5 K}{1 + K} \quad (3)$$

the turning point should correspond to 50% hydrogen transfer, that is at the $\text{p}K_{\text{a}}$ of the acid HTMPPO^+ . In eqn. (3), 13.9 is the phosphorus-31 chemical shift when no phenol hydrogen donor is linked to the TMPPO residue, 39.5 is the maximum chemical shift obtained for the most acidic phenol, picric acid, and K is given by eqn. (4). However, to the best of our knowledge, no

$$K = \frac{K_{\text{a}}\text{phenol}}{K_{\text{a}}\text{HTMPPO}^+} \quad (4)$$

$\text{p}K_{\text{a}}$ has been previously assigned to HTMPPO^+ . From the results obtained by solution-state studies this $\text{p}K_{\text{a}}$ value should lie between 2 and 4. Hence, a $\text{p}K_{\text{a}} = 3$ is estimated in order to perform calculations according to eqn. (3). Fig. 2 displays solution-state ^{31}P chemical shifts obtained as a function of the $\text{p}K_{\text{a}}$ of the phenol. The dotted curve represents the theoretical sigmoidal according to eqn. (3) and the solid circles are the experimental data. No points are displayed in Fig. 2 for 2,6-dinitrophenol–TMPPO and dichloro-4-nitrophenyl–TMPPO since in these cases there is no hydrogen transfer (see below). When analysing the experimental ^{31}P chemical shifts for the complexes in solution, good agreement is obtained with respect to the theoretical line.

Solid-state studies

To determine if phenol–TMPPO systems exhibit the same behaviour in the solid state as in solution, we first focus on changes produced by the hydrogen transfer on the chemical shifts of the phenol carbons at positions 1 and 4. This effect is a consequence of the increased contribution of structures in which the phenol ring has a negative charge while the hydroxylic proton moves apart from the oxygen atom. Therefore, C1 is influenced by a higher C–O double-bond order and, in some of the contributing structures, C4 carries a formal negative charge. The result of this situation is that the C1 and C4 chemical shifts change in an opposite manner, C1 becoming more deshielded and C4 more shielded, as compared with the values in the free phenols. Table 2 displays the solid-state ^{13}C chemical shifts of the relevant nuclei for pure phenol and for the phenol–TMPPO complexes, as well as Δ_{1-4} calculated values. As has already been described, some phenols possess an intramolecular hydrogen bond between the substituent in position 2 or 6 and the hydroxylic proton of the phenol.⁹ In these cases, an experimental correction factor (5.1 ppm) has to be added to the experimental Δ_{1-4} values in order to compensate for the shift in the C1 and C4 signals for those phenols in solution.¹⁷ The same correction has also been suggested for complexes in the solid phase, on the basis of the reported crystal structure of some pure substituted phenols, where it is known that *intra*-molecular hydrogen bonding is present.¹⁴ From Table 2 it can be seen that Δ_{1-4} decreases as long as the $\text{p}K_{\text{a}}$ of the substituted phenol increases, indicating a relative reduction in the extent of the acid–base reaction. There is an exception for this behaviour, exhibited by the 2,6-dichloro-4-nitrophenol complex, which displays a corresponding Δ_{1-4} of 3.6 ppm. This value suggests that there is negligible hydrogen transfer. In spite of the low $\text{p}K_{\text{a}}$ of this phenol, in the solid state there is no possibility for the hydroxylic proton to be transferred from the phenol to the TMPPO residue, for steric reasons, as has been observed in the solution state.

The behaviour of the set of crystalline adducts was also

Table 3 Relevant solid-state ^{31}P NMR data for TMPPO–phenol complexes and for tris(2,4,6-trimethoxy)phenylphosphine oxide (TMPPO)

Compound	δ_{iso} (ppm)		$(^a\sigma_{\perp} - \sigma_{\text{iso}})^b$ (ppm)		$(\sigma_{\parallel} - \sigma_{\text{iso}})^b$ (ppm)		$\Delta\sigma^{c,d}$ (ppm)	
	Unhydrated	Hydrated	Unhydrated	Hydrated	Unhydrated	Hydrated	Unhydrated	Hydrated
Picric acid–TMPPO	—	41	—	–35	—	70	—	105(2)
2,4-Dinitrophenol–TMPPO	16	—	–55	—	112	—	167(2)	—
2,5-Dinitrophenol–TMPPO	15	23	–57	–50	114	100	171(2)	150(1)
4-Nitrophenol–TMPPO	—	21	—	–55	—	110	—	165(2)
4-Chlorophenol–TMPPO	11	19	–62	–59	124	118	186(1)	177(1)
Phenol–TMPPO	9	18	–62	–60	124	120	186(4)	180(1)
4-Methoxyphenol–TMPPO	9	—	–63	—	126	—	189(1)	—
TMPPO (pure)	6	11	–74	–69	148	138	222(1)	207(3)

^a $\sigma_{\perp} = \sigma_{11} = \sigma_{22}$. ^b Shielding data are presented using the sign convention opposite to that used for δ_{iso} . ^c $\Delta\sigma = \sigma_{\parallel} - \sigma_{\perp}$. ^d The errors are those given by the computer program²⁰ for the sideband analysis. They probably underestimate the real errors which arise from experimental matters.

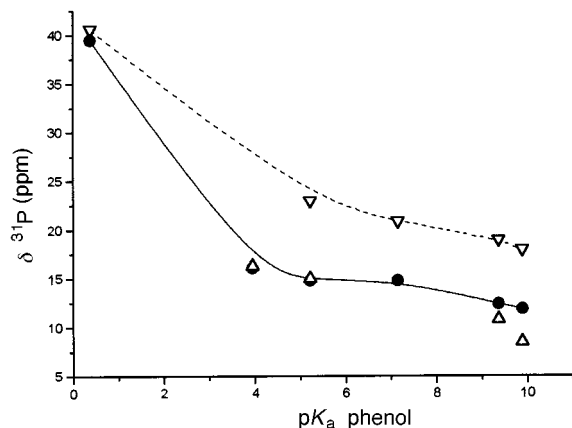


Fig. 3 Comparison between solution- and solid-state ^{31}P NMR results for the complexes, as a function of $\text{p}K_{\text{a}}$ for the phenols; \bullet = $\delta^{31}\text{P}$ values for complexes in chloroform solution; ∇ and \triangle = phosphorus-31 δ_{iso} values for solid-state complexes (hydrated and unhydrated, respectively) obtained by CPMAS experiments

studied by means of high-resolution solid-state ^{31}P NMR experiments. The results are presented both in Fig. 3, which compares the performance between solution- and solid-state complexes, and in Table 3, which displays the relevant data for the crystalline adducts. Fig. 3 shows the variation of the phosphorus-31 isotropic chemical shift, δ_{iso} , in the solid state as a function of the $\text{p}K_{\text{a}}$ of the phenol, as compared with phosphorus chemical shifts observed in solution for the same set of complexes. It is apparent that the pattern followed by the TMPPO–phenol adducts in the solid state is essentially the same as that in solution.

The crystal structure of pure TMPPO has already been determined by X-ray diffraction, and it has been shown that this oxide exists as at least three solid forms.²¹ The one crystallised by slow evaporation from a dichloromethane–hexane solvent mixture is the first triclinic form, which has two different TMPPO molecules per crystallographic asymmetric unit. One of the oxide moieties has a water molecule hydrogen-bonded, and the other oxide molecule has no such linkage. It has been suggested that the origin of the crystallisation water may be the use of aqueous hydrogen peroxide to carry out the oxidation of the phosphine.²² Even though TMPPO is exposed to a high vacuum, the hydration water is not totally removed. As a consequence, the solid-state ^{31}P NMR spectrum of this compound gives two different signals, one corresponding to the water-linked molecule with $\delta_{\text{iso}} = 11$ ppm, and the other corresponding to the unhydrated molecule with $\delta_{\text{iso}} = 6$ ppm. In turn, the number of ^{31}P signals obtained for the solid-state complexes varies depending on the particular adducts. Fig. 4 illustrates the ^{31}P spinning sideband manifold for pure TMPPO together with that obtained for the picric acid–TMPPO complex. Some of the adducts show two different phosphorus signals (the phenol, 2,5-

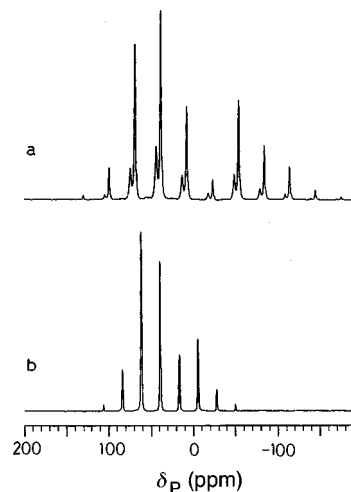


Fig. 4 Phosphorus-31 spinning sideband manifolds obtained at 81.015 MHz for: (a) pure TMPPO with 5.0 ms contact time, 6.0 s pulse delay, 32 transients and spinning speed 2500 Hz; (b) the picric acid–TMPPO complex with 5.0 ms contact time, 8.0 s pulse delay, 32 transients and spinning speed 1800 Hz

dinitrophenol and 4-chlorophenol derivatives), and the same holds true for pure TMPPO. The other complexes studied have only one signal (picric acid, 2,4-dinitrophenol, 4-nitrophenol and 4-methoxyphenol derivatives). A clearer understanding of this phenomenon arises when the previously described structure of pure TMPPO is taken into account. Thus, it may be reasonably expected that water molecules hydrogen-bonded into complexes would cause similar effects on the oxide moiety to those observed for pure TMPPO hydrate crystals. Following the idea pointed out by Harrison,²¹ it might be assumed that the different phosphorus signals arise from different extents of hydrogen bonding due to distinct amounts of water hydrating the oxide. Table 3 displays the relevant ^{31}P parameters for the complexes studied and for pure TMPPO. All the isotropic ^{31}P NMR shifts of the complexes are deshielded as compared with pure TMPPO. In addition, a displacement towards the free TMPPO δ_{iso} value as the $\text{p}K_{\text{a}}$ of the phenol increases is observed. This behaviour is easily understood, since the isotropic chemical shift varies with the electron density around a nucleus, which is indeed expected to change with the degree of hydrogen transfer. A detailed analysis of the shifts of the phosphorus signals leads to a differentiation between two groups of signals, one with δ_{iso} values that correlate with hydrated TMPPO residues and the other group related to unhydrated TMPPO moieties. The difference between ^{31}P δ_{iso} values for the hydrated TMPPO residue in the pure oxide and its counterpart, *i.e.* the unhydrated molecule, is 5 ppm. Surprisingly, the difference found for the adducts which present two different phosphorus signals turns out to be almost the same for all of them (8 ppm, see Table 3). Hence, it could be assumed that this

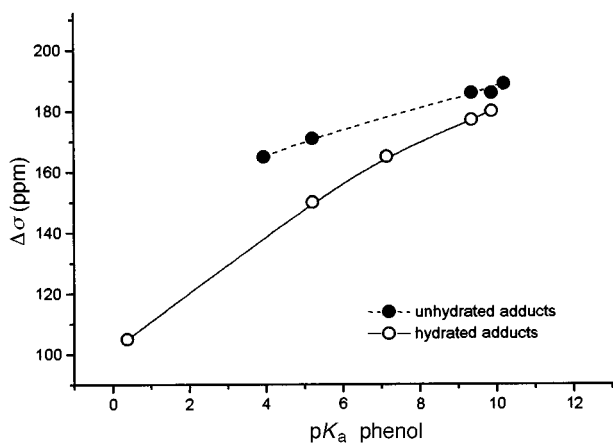


Fig. 5 Phosphorus $\Delta\sigma$ values for the solid-state complexes as a function of the pK_a of the phenols

difference in δ_{iso} is the result of the same effect on every complex, this being the influence exerted by the hydration water linked to the TMPPO residue in the adduct. To help assess the validity of this hypothesis, we tried to find supporting evidence by studying other parameters obtained by measuring the components of the phosphorus-31 shielding tensor.

As discussed in earlier work, the ^{31}P shielding tensor components (σ_{ii}), anisotropy ($\Delta\sigma$) and the asymmetry (η)^{14,23-27} are highly sensitive parameters that reflect changes in the surroundings of the phosphorus nucleus. It should be noticed that changes in phosphorus-31 δ_{iso} values occupy a smaller range than $\Delta\sigma$ for the same complexes, showing the enhanced sensitivity of the latter parameter (see Table 3). In all these compounds, the asymmetry is zero, indicating that all oxide residues are axially symmetric within experimental error not only in pure TMPPO but also in the adducts. Spinning sideband manifolds are, however, insensitive^{20,28,29} to values of η less than ca. 0.2. The anisotropies of each type of phosphorus nucleus for pure TMPPO are 207 and 212 ppm, the former corresponding to the hydrated moiety and the latter for the residue that is not linked to water.²² Fig. 5 illustrates $\Delta\sigma$ values of the complexes as a function of the pK_a of the phenol. For complexes giving rise to two phosphorus signals, both anisotropy values increase as the pK_a of the substituted phenol increases, following the tendency discussed previously for the isotropic chemical shift. In line with previous reports,^{7,30-32} this is the predicted outcome of a relatively more asymmetric environment of the phosphorus nucleus. The change in the anisotropy values is controlled by relative differences among individual π P–O bond orders.³² Hence, the described increase of $\Delta\sigma$ accompanies the increase of π electron density along the involved bond produced by a smaller contribution of the $(\text{TMPPO-H})^+$ structure with weaker proton donors. Thus, this effect should be the result of a smaller degree of hydrogen transfer when the substituted phenol increases its pK_a value. Therefore, the principal components of the ^{31}P shielding tensor assume values corresponding to a more tetrahedral phosphorus environment as the pK_a of the phenol increases.

Taking into account the crystal structure of TMPPO, in which the hydrated molecule of the oxide gives a smaller value of $\Delta\sigma$, it is reasonable to infer that, in complexes presenting two different values of anisotropy, the smaller one would correspond to a hydrated oxide moiety. Of course, $\Delta\sigma$ values for both hydrated and unhydrated complexes should vary as a function of pK_a of the phenol. This change has to be as discussed previously, *i.e.* $\Delta\sigma$ values for the adducts should increase as the extent of the hydrogen transfer reaction diminishes. However, anisotropies of hydrated TMPPO residues in the complexes should tend to a higher value than those of unhydrated TMPPO moieties since pure water-linked oxide has

$\Delta\sigma = 212$ ppm, whereas the anisotropy for the unhydrated oxide has 207 ppm, *i.e.* to the values for the uncomplexed TMPPO (Fig. 5). The difference between $\Delta\sigma$ (unhydrated minus hydrated) in the pure oxide is 5 ppm. Complexes with two distinct phosphorus signals have shown an increasing difference between the anisotropy values as the pK_a of the phenol decreases (6 ppm for phenol–TMPPO to 21 ppm for 2,5-dinitrophenol–TMPPO, see Table 3). Comparing the anisotropy differences for the solid complexes which have two phosphorus signals with the differences between δ_{iso} ^{31}P values, the higher sensitivity displayed by the former parameters as compared with their isotropic counterparts becomes more apparent.

Conclusions

The hydrogen transfer process has been studied in a number of complexes between substituted phenols and TMPPO. Proton and phosphorus-31 NMR spectroscopies have been the chosen methodologies to monitor the behaviour of the adducts in the solution state, while high-resolution CPMAS ^{13}C and ^{31}P NMR have been used to study them in the solid phase. The complexes show the same variation pattern in the two phases. The acid–base reaction seems to have a larger extent as the pK_a of the substituted phenol decreases. The evidence supporting this hypothesis is that the phenolic ^1H NMR signal moves to higher frequencies. The shifting continues until the proton is substantially transferred from the phenol to the oxide residue (picric acid complex). On the other hand, $\delta^{31}\text{P}$ for the complexes in solution showed the same trend, its value increasing as the acidity of the phenolic hydrogen increases. The adducts studied in the solid state showed a reduction of the ^{31}P shielding anisotropy with the acid strength of the associated phenol, while ^{13}C NMR results displayed higher shift differences between phenolic C1 and C4 signals with decreasing pK_a values.

Acknowledgements

Robin M. Harrison is gratefully acknowledged for useful comments on crystallographic data. C. M. L. and A. C. O. acknowledge Universidad Nacional de Rosario, the British Council and Fundación Antorchas for financial support.

References

- 1 P. Schuster, G. Zundel and C. Sandorfi, *The Hydrogen Bond, Recent Developments in Theory and Experiments*, North Holland, Amsterdam, 1976.
- 2 T. L. Brown, L. G. Butler, D. Y. Curtin, Y. Hiyama, I. C. Paul and R. B. Wilson, *J. Am. Chem. Soc.*, 1982, **104**, 1172.
- 3 J. Emsley, *Struct. Bonding (Berlin)*, 1984, **56**, 147.
- 4 F. Herstein, M. Kapon, G. M. Reisner, M. S. Lehman, R. B. Kress, R. B. Wilson, W. I. Shiau, E. N. Duesler, I. C. Paul and D. Y. Curtin, *Proc. R. Soc. London, Ser. A*, 1985, **399**, 295.
- 5 D. R. Clark, J. Emsley and F. Hibbert, *J. Chem. Soc., Chem. Commun.*, 1988, 1252.
- 6 A. J. Vila, C. M. Lagier and A. C. Olivieri, *J. Chem. Soc., Perkin Trans. 2*, 1990, 1615.
- 7 C. M. Lagier and A. C. Olivieri, *Solid State NMR*, 1994, **3**, 163.
- 8 C. M. Lagier, M. Zuriaga, G. Monti and A. C. Olivieri, *J. Phys. Chem. Solids*, 1996, **57**, 1183.
- 9 M. Ilczyszyn, Z. Latajka and H. Ratajczak, *Org. Magn. Reson.*, 1980, **13**, 132.
- 10 B. Brycki, Z. Szafran and M. Szafran, *Pol. J. Chem.*, 1980, **54**, 221.
- 11 B. Brycki and M. Szafran, *J. Chem. Soc., Perkin Trans. 2*, 1982, 1333.
- 12 B. Brycki and M. Szafran, *J. Chem. Soc., Perkin Trans. 2*, 1984, 223.
- 13 T. Keil, B. Brzezinski and G. Zundel, *J. Phys. Chem.*, 1992, **96**, 4421.
- 14 C. M. Lagier, U. Scheler, G. McGeorge, M. G. Sierra, A. C. Olivieri and R. K. Harris, *J. Chem. Soc., Perkin Trans. 2*, 1996, 1325.
- 15 F. Guilan, J. P. Senguin, L. Nadjro, R. Uzan, F. Membrey and J. P. Doucet, *J. Chem. Soc., Perkin Trans. 2*, 1984, 1139.
- 16 M. Ilczyszyn, H. Ratajczak, Z. Latajka and K. Skowronek, *Magn. Reson. Chem.*, 1988, **26**, 445.

- 17 B. Brycki, B. Brzezinski, G. Zundel and T. Keil, *Magn. Reson. Chem.*, 1992, **30**, 507.
- 18 M. Wada and S. Higashizaki, *J. Chem. Soc., Chem. Commun.*, 1984, 482.
- 19 D. Fenzke, B. Maess and H. Pfeifer, *J. Magn. Reson.*, 1990, **88**, 172.
- 20 A. C. Olivieri, *J. Magn. Reson.*, 1996, **123**, 207.
- 21 (a) P. A. Chaloner, R. M. Harrison and P. B. Hitchcock, *Acta Crystallogr., Sect. C*, 1993, **49**, 1072; (b) K. R. Dunbar and S. C. Haefner, *Polyhedron*, 1994, **13**, 727.
- 22 R. M. Harrison, *Synthesis and structural studies of novel organophosphorus compounds for second harmonic generation*, Ph.D. Thesis, University of Sussex, 1993.
- 23 A. R. Grimmer, *Spectrochim. Acta, Part A*, 1978, **34**, 941.
- 24 M. Mehring, *High Resolution NMR in Solids*, Springer-Verlag, Berlin, 1983.
- 25 G. L. Turner, K. A. Smith, R. J. Kirkpatrick and E. Oldfield, *J. Magn. Reson.*, 1986, **70**, 408.
- 26 N. E. Burlinson, B. A. Dunell and J. A. Ripmeester, *J. Magn. Reson.*, 1986, **67**, 217.
- 27 J. C. Facelli and D. M. Grant, *Top. Stereochem.*, 1989, **19**, 1.
- 28 N. J. Clayden, C. M. Dobson, L. Y. Lian and D. J. Smith, *J. Magn. Reson.*, 1986, **69**, 476.
- 29 R. K. Harris, P. Jackson, L. H. Merwin, B. J. Say and G. Hägele, *J. Chem. Soc., Faraday Trans. 1*, 1988, **84**, 3469.
- 30 A. J. Vila, C. M. Lagier, G. Wagner and A. C. Olivieri, *J. Chem. Soc., Chem. Commun.*, 1991, 684.
- 31 C. M. Lagier, A. C. Olivieri, D. C. Apperley and R. K. Harris, *Solid State NMR*, 1992, **1**, 205.
- 32 A. C. Olivieri, *J. Magn. Reson.*, 1990, **88**, 1.
- 33 R. K. Harris, M. M. Sünnetçioğlu, K. S. Cameron and F. G. Riddell, *Magn. Reson. Chem.*, 1993, **31**, 963.
- 34 R. M. Cravero, C. Fernandez, M. Gonzalez-Sierra and A. C. Olivieri, *J. Chem. Soc., Chem. Commun.*, 1993, 1253.

Paper 8/02219D
Received 20th March 1998
Accepted 1st June 1998